Generating a Quasiellipsoidal Electron Beam by 3D Laser-Pulse Shaping

Yuelin Li[1,2] and John W. Lewellen[2,3]

[1]*Accelerator Systems Division, Argonne National Laboratory, Argonne, Illinois 60439, USA*
[2]*Argonne Accelerator Institute, Argonne National Laboratory, Argonne, Illinois 60439, USA*
[3]*Argonne ONR Project Office, Argonne National Laboratory, Argonne, Illinois 60439, USA*

(Received 22 March 2007; published 19 February 2008)

A generic 3D laser-pulse-shaping scheme is proposed towards the generation of a uniform ellipsoidal particle distribution, an ideal distribution due to the linear dependence of the space-charge force on the particle position. The shaping is accomplished via spatiotemporal coupling of the laser dynamics via chromatic aberration in an optical lens. Particle tracking simulations show that the electron beam initiated by such a laser pulse in a high-gradient radio-frequency photoinjector delivers very low emittance, ideal for beam-based light sources such as the x-ray free-electron laser.

DOI: 10.1103/PhysRevLett.100.074801 PACS numbers: 29.27.Bd, 29.27.Eg, 41.75.Ht, 42.60.Jf

X-ray free-electron lasers (XFELs) are now under construction in the U. S. and in Europe [1,2]. Because of their unprecedented coherence, brightness, and short pulse duration, they are envisaged to open a new horizon for femtochemistry, nanoscale dynamics in material science, and molecular biological science [3]. These x-ray free-electron lasers require short, high-brightness electron bunches that are typically obtained from a photoinjector. The desired charge is on the order of 1 nC and the emittance must be less than 1 mm mrad. The benefit of simultaneously having a high beam change and a low beam emittance in an XFEL is that the beam energy or the number of undulators can be reduced, thus making for a more efficient facility. Electron bunches of this quality or better are also indispensable for ultrafast electron diffraction experiments and time resolved electron microscope [4], and other beam-based light source facilities such as energy recovery linacs [5].

According to the laws of physics, however, high charge and low emittance are naturally conflicting goals, as can be seen from the definition of the emittance:

$$\varepsilon = \sqrt{\langle x^2\rangle\langle x'^2\rangle - \langle xx'\rangle^2}. \quad (1)$$

Here the brackets denote averaging over the particle ensembles, and x and x' are the transverse phase space coordinates. As $x' \propto p_x \propto E_s \propto C/\gamma^2\beta$ (where γ, β, and C are the relativistic factor, the speed of the particle, and the beam current, respectively), the emittance can grow significantly at low γ with high current while at large γ the emittance is frozen. To solve this problem, the theory of emittance compensation was developed [6,7] and one of the results of this theory is that the emittance growth due to the linear portion of the space-charge force can be fully recovered. Thus a 3D Kapchinskij and Vladimirkij distribution [8] or a uniform ellipsoidal (UE) beam, with only linear space-charge field [9], is a highly desirable beam distribution.

Because of technical difficulties in realizing a UE beam, however, a uniform cylindrical (UC) beam is proposed for the XFELs [1,2] and other applications. The suggestion of ultilizing space-charge blowout [10] and the refined "recipe" [11] have sparked a new excitement for generating a UE beam. In the recipes [11,12], a very thin pancake beam initialized by an ultrashort laser pulse (<30 fs) with proper transverse profile is expected evolve into a UE beam. However, the scheme breaks down at larger charges due to the image charge field in the vicinity of the cathode [11,13].

To mitigate image charge effects at high beam charge, one possibility is to apply a UE laser pulse to the cathode: simulation [14] for the XFELs has shown clear advantages of the UE pulse over a UC pulse. However, generating a UE pulse remains a challenge [14]. The difficulty arises from the requirement of full spatiotemporal control of the pulse while the existing shaping techniques normally work independently in either the time [15,16] or space domain [17]. Spatiotemporal control via structured optical elements [18] is complicated and needs further exploration.

In this Letter, we present a generic scheme for generating a quasi-UE laser pulse that gives a beam emittance approaching that of an ideal UE pulse. The scheme is based on the coupling of spatiotemporal dynamics of a broadband laser in a chromatic focusing lens. The dependence of the refractive index upon the optical frequency in a chromatic lens gives rise to the well-known chromatic aberration [19] $1/f(\omega) = [n(\omega) - 1](1/R_1 - 1/R_2)$. Here f is the focal length; R_1, R_2 are the radius of curvature of its front and back surfaces, respectively; and n is the refractive index. The change of the focal length δf due to a shift in frequency $\delta\omega$ is

$$\delta f = -\frac{f_0}{n_0 - 1}\chi\delta\omega, \quad (2)$$

where f_0 is the nominal focal length at ω_0. We assume that the frequency shift is small, hence $\chi = dn/d\omega$ is constant. For a Gaussian beam, the beam size at the nominal focal plane is [19]

$$w \approx w_0\left[1+\left(\frac{\delta f}{z_R}\right)^2\right]^{1/2}. \quad (3)$$

Here $w_0 = N\lambda_0/\pi$ is the beam waist at the nominal wavelength λ_0, with N the numerical aperture, and $z_R = \pi w_0^2/\lambda_0$ is the Rayleigh range. It is obvious from Eqs. (2) and (3) that, if one can program $\delta\omega$ in time, a time-dependent beam size can be controlled. For $\delta\omega(t) = \omega(t) - w_0$, $w(t) \cong |\delta f(t)|/N$ at $\delta f \gg z_R$. To generate an ellipsoidal envelop with maximum radius of R and full length of $2T$, the transverse beam size as a function of time is $w(t) = R[1-(t/T)^2]^{1/2}$, which in turn gives the frequency shift as a function of time as $|\delta\omega(t)| = \Delta\omega[1-(t/T)^2]^{1/2}$. Here $\Delta\omega = (n_0-1)NR/\chi f_0$ is the maximum frequency shift. The phase of the pulse is therefore

$$\phi(t) = \int[\omega(t)-\omega_0]dt = -\omega_0 t \pm \frac{\Delta\omega}{2}\left\{t\left[1-\left(\frac{t}{T}\right)^2\right]^{\alpha} + T\sin^{-1}\frac{t}{T}\right\}, \quad (4)$$

where $\alpha = 1/2$. To keep the laser flux $|A(t)|^2/w(t)^2$ constant over time, we have

$$A(t) = A_0\left[1-\left(\frac{t}{T}\right)^2\right]^{\eta}, \quad (5)$$

with $\eta = 1/2$. Equations (4) and (5) represent a laser pulse that is expected to generate a UE flux distribution at the focal plane of a lens. However, the above analysis cannot treat the diffraction and other dispersion effects such as group velocity delay (GVDE) and group velocity dispersion (GVDI), which are critical for broadband laser-pulse manipulation. These effects are numerically evaluated using a Fourier optics model, elaborated in Ref. [20], in which the field distribution at the focal plane can be calculated in the frequency domain and then Fourier transformed back into the time domain:

$$U(r,\omega) = \int_0^p \rho d\rho \int_0^{2\pi} d\theta u(\omega)\Gamma(\rho,\omega) \times \exp(-jk_a\sqrt{f_0^2+\rho^2+r^2-2\rho r\cos\theta}). \quad (6)$$

Here $u(\omega) = F\{A(t)\exp[-j\phi(t)]\}$ is the Fourier transform of the input pulse, P, ρ, and θ are the lens radius, the ray location, and the azimuthal angle, respectively. Γ is the lens transfer function:

$$\Gamma(\rho,\omega) = \exp\left(jk_l d + j\frac{k_a}{2f_0}\rho^2\right) \times \exp\left[-j(k_l-k_a)\frac{\rho^2}{2(n-1)f_0}\right]. \quad (7)$$

Here $k_l = nk_a$ and $k_a = \omega/c$ are the wave numbers in the lens and in air, respectively. We assume a circular input beam with a uniform spatial profile.

In fact, the GVDE and diffraction effects prevent us from generating a perfect UE pulse, and α and η are adjusted in Eqs. (4) and (5) for better emittance. The time and frequency domain representation of a pulse with excellent performance is shown in Figs. 1(a) and 1(b), with $T = 6$ ps, $\lambda_0 = 0.25$ μm, and $\Delta\omega/\omega = 8\%$. The spatiotemporal flux at the focal plane of an $f_0 = 150$ mm fused silica lens is given in Fig. 1(c).

The intensity in Fig. 1(c) displays the basic features of a UE pulse but with noticeable distortions. Most prominent is the recess in the leading edge and the protrusion at the trailing edge due to the group delay between rays traversing the lens at different radii, with the maximum delay of $\Delta t = -\mathrm{P}^2\lambda\frac{dn}{d\lambda}/2cf(n-1)$ [20] and is determined by the lens parameters. With longer pulses, the impact can be much reduced. The distribution also displays diffractions. The detail of the structure also depends on the laser bandwidths. The pulse can be image relayed onto the cathode using achromatic optics to maintain the temporal-spatial fidelity.

To analyze the dynamics of a beam initiated by such a laser pulse, we generate a quasi random particle distribution with minimized statistic noise, shown in Fig. 2(a), using a Hammersley series [21]. The transverse dimension is scaled to $R = 1$ mm. The calculation of particle dynamics includes 10^5 macroparticles representing 1 nC of charge and is performed using the code GPT [22]. A nonequidistant mesh is used to solve the Poisson equation.

The transverse space-charge field distribution in free space is plotted in Fig. 2(b) in comparison with that of a UE beam, which is linear [9]. The shaped beam shows an obvious deviation from the linear distribution. However, due to the cathode image charge and other dynamic effects, the beam leaving the cathode can assume a different distribution from the laser flux distribution. To analyze this,

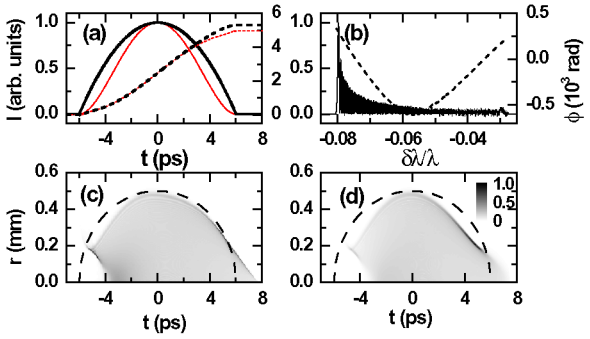

FIG. 1 (color online). (a) Time and (b) frequency domain representation (heavy solid line: intensity; heavy dashed line: phase), and (c) the spatiotemporal intensity distribution of a laser pulse that gives an excellent emittance [$\alpha = 1/2$ at $t < 0$, and $\alpha = 1$ at $t \geq 0$, and $\eta = 1/2$ in Eqs. (4) and (5)]. The pulse has a 5% full bandwidth at 249 nm (about 1% full width at half maximum). The thinner lines in (a) represent a pulse with significant error in amplitude (solid) and phase (dashed) [$\alpha = 1$ and $\eta = 1$ in Eqs. (4) and (5)], and (d) is its intensity distribution. A $P = 25$ mm and $f = 150$ mm fused silica lens is used. The dashed lines in (c) and (d) are the edge of an ideal ellipsoid.

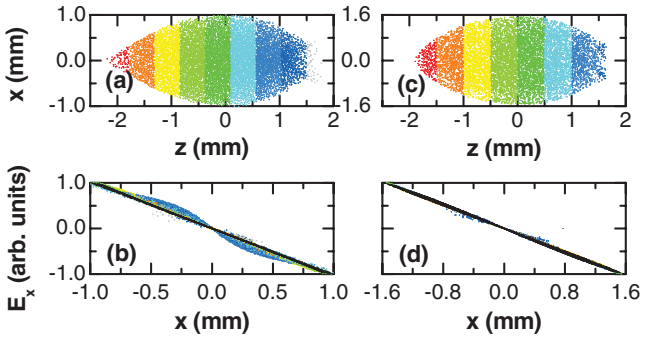

FIG. 2 (color). Particle distribution projected onto the z-x plane and space-charge field distribution for the shaped (colored) and an ideal ellipsoidal (black) laser beam case: (a, b) in free space; (c, d) 2.4 cm away from the cathode in the rf gun. The field plots are color coded by the z position of the particles for the shaped laser case as shown in (a) and (c).

we use the injector setup [23] for the Linac Coherent Light Source (LCLS) [1], one of the XFELs under construction. The injector consists of a 1.6-cell rf gun at 2856 MHz, a solenoid, a drift space, and two 3-m traveling-wave linacs starting at 1.5 m from the cathode. We use 140 MV/m gun and 35 MV/m linac gradients [23]. The UC and UE laser pulses are used to benchmark the result. The parameters and the optimized injector setting are listed in Table I. To reveal the effect of the beam geometry, optimization is performed without the thermal emittance (see below).

Figures 2(c) and 2(d) depict the particle and the space-charge field distributions extracted from the shaped case after a propagation of 2.4 cm from the cathode. Interestingly, the particle distribution is more ellipsoidal in comparison with that in Fig. 2(a). Furthermore, the space-charge field distribution [Fig. 2(d)] narrows significantly in comparison with that in Fig. 2(b). In contrast, for the UE case, the space-charge field distribution broadens somewhat.

TABLE I. The 1-nC beam parameters and the optimized accelerator setting for gun and linac phase ϕ, ϕ_{linac}, and solenoid field B. The final transverse beam size σ_x and longitudinal emittance ε_z are also given. Superscript t and d denote cases with thermal emittance and phasing errors, respectively.

Beam	Shaped	UE	UC	PC
R (mm)	1	1	1	1
T_{Full} (ps)	12	12	10	0.1 rms
ε_x (10^{-6} m rad)	0.38	0.36	0.61	0.86
	0.57^t	0.57^t	0.79^t	0.95^t
	$0.65^{t,d}$		$0.95^{t,d}$	
σ_x (mm)	0.8	0.6	1.3	0.75
ε_z (10^{-7} eV s)	6.2	6.4	4.8	1.4
ϕ	27.4°	32°	40°	27.5°
B (T)	0.3122	0.311	0.31	0.31
ϕ_{linac}	45°	20°	−42°	0°

Figures 3(a) and 3(b) give the evolution of the beam size σ_x and emittance ε_x as functions of propagation distance without the booster linac at the optimized setting. For the UC case, the result in [23] is reproduced, showing double emittance minima and a laminar beam waist corresponding roughly to the local emittance maximum. The shaped case also demonstrates the double emittance minima. For the UE case, in contrast, only one emittance minimum is seen. The laminar beam waists are located approximately at the linac entrance of $z = 1.5$ m, fulfilling the invariant envelop requirement for emittance compensation [7].

After capture by the linac, the emittance starts to cascade down as pictured in Fig. 3(c). The emittances at 10 m from the cathode are listed in Table I. With zero thermal energy, the emittance for the shaped and UE case are $\varepsilon_x = 0.38$ and 0.36 mm mrad and represent 38% and 40% reduction from the UC case of $\varepsilon_x = 0.61$ mm mrad, respectively. The emittance for the pancake (PC) scheme is minimized at 0.86 mm mrad, due to the severe distortion of the final beam geometry. When including an initial electron energy of 0.775 eV with a half-sphere momentum distribution, the emittance becomes 0.57, 0.57, 0.79, and 0.95 mm mrad for the UE, shaped, UC, and PC cases, respectively. Again, the performance of the shaped pulse closely matches that of the UE pulse and is significantly better than that of the UC pulse. Note that with thermal energy, the initial emittance is 0.5 mm mrad for the UC beam but smaller for the other beam geometry at about 0.45 mm mrad. The UE case is more robust when errors in the accelerator setting are considered (Fig. 4).

The excellent performance of the shaped pulse might be the result of the image charge effect that apparently improves the particle distribution for the shaped pulse but causes distortion for the UE pulse, evidenced by the space-charge field distribution in Fig. 2(b)–2(d). This is further evidenced in simulations for 0.1 nC charges, where the image charge effect is significantly reduced and the difference between the optimized emittance is widened considerably, at 0.05 and 0.12 mm mrad (no thermal emittance) for the UE and the shaped pulse, respectively. The dynamics of this apparent self compensation remains to be elucidated.

The phase in Eq. (4), though apparently complicated, is dominated by the common third order phase that can be

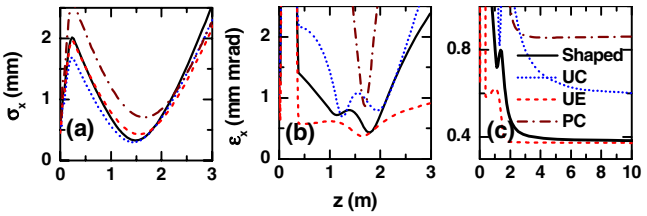

FIG. 3 (color online). (a) Transverse beam size and (b) emittance as functions of propagation distance at optimal launch phase and solenoid field without the booster linac; (c) beam emittance as a function of propagation distance with the booster linac for different laser-pulse shapes. Thermal emittance is not included nm here.

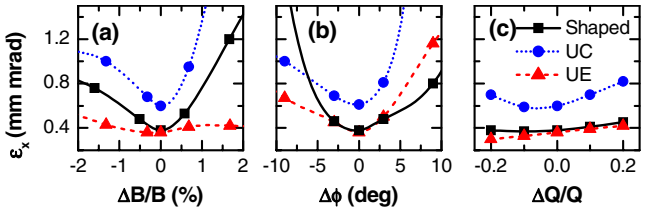

FIG. 4 (color online). Beam emittance at the end of the booster linac as a function of (a) solenoid field error, (b) the launch phase error, and (c) the charge fluctuation. Thermal emittance is not included here.

generated via self-phase modulation and is exploited in various laser applications. For precise control, one of the possible practical but not necessarily trivial solutions is the acousto-optic programmable dispersive filter (AOPDF) [16]. AOPDF uses the transient Bragg effect in a crystal induced by an acoustic wave to manipulate the phase and amplitude of a laser pulse. In comparison with the effort using an AOPDF to generate a UC pulse [24], a more precise amplitude control is expected in our case as the ripples associated with the cut-off due to the finite crystal length are minimal because the signal goes more smoothly to zero at the edges. Indeed, using the waveform and phase in Fig. 1(a) as input, an AOPDF simulation reproduced the spectrum in Fig. 1(b) with an error smaller than 0.1% [25]. Though it is difficult to pinpoint the effect of a variety of shaping errors, we note that the edge sharpness in our case is mostly defined by the edge sharpness of the input beam, in contrast to the case for a cylindrical beam where the phase error directly maps into the sharpness of the rising and falling edges. A typical 1-ps rising and falling edge of a cylindrical pulse [24] increases the emittance significantly, from 0.79 to 0.95 mm mrad (with thermal emittance) in our simulation. Simulation for a shaped pulse with significant error in both phase and amplitude [depicted in Figs. 1(a)–1(d)] shows an increase of emittance from 0.57 to 0.65 mm mrad (with thermal emittance). We also note that the emittance of 0.95 mm mrad for the distorted UC beam is very close to the recently measured value of 1.1–1.3 mm mrad [26].

In conclusion, the generic 3D shaping scheme generates quasiuniform ellipsoidal laser pulses that initiate beams with emittance approaching that of an ideal uniform ellipsoidal pulse. The shaping can be implemented using the techniques such as AOPDF and is robust against shaping errors. Further optimization of the laser pulse and adoption of more complex compensation schemes [23,27] is possible, but this involves a larger parameter space and thus needs sophisticated optimization algorithms such as the one used for a DC photoinjector [28].

We thank D. Kaplan of Fastlite for fruitful discussions and data exchange. Technical help of Pulsar Physics is acknowledged. The authors also thank K.-J. Kim and K. Harkay for support. This work is supported by the U. S. Department of Energy, Office of Science, Office of Basic Energy Sciences, under Contract No. DE-AC02-06CH11357.

[1] M. Cornacchia *et al.*, SLAC Report No. SLAC-R-521 (Stanford Linear Accelerator Center, Stanford, CA), revised 1998.
[2] DESY Report No. DESY97-048 (Deutsches Elektronen-Synchrotron, Hamburg), 1997.
[3] See, for example, LCLS the first experiments, SLAC Report No. SLAC-R-611 (Stanford Linear Accelerator Center, Stanford, CA), 2003, and references therein.
[4] See W. E. King *et al.*, J. Appl. Phys. **97**, 111101 (2005), and references therein.
[5] S. M. Grunner *et al.*, Rev. Sci. Instrum. **73**, 1402 (2002).
[6] B. E. Carlsten, Nucl. Instrum. Methods Phys. Res., Sect. A **285**, 313 (1989).
[7] L. Serafini and J. B. Rosenzweig, Phys. Rev. E **55**, 7565 (1997).
[8] I. M. Kapchinskij, V. V. Vladimirskij, *Conference on High Energy Accelerators and Instrumentation* (CERN, Geneva, 1959), p. 274.
[9] M. Reiser, *Theory and Design of Charged Particle Beams* (Wiley, New York, 2005).
[10] L. Serafini, AIP Conf. Proc. **413**, 321 (1997).
[11] O. J. Luiten *et al.*, Phys. Rev. Lett. **93**, 094802 (2004).
[12] B. J. Claessens *et al.*, Phys. Rev. Lett. **95**, 164801 (2005).
[13] J. B. Rosenzweig *et al.*, Nucl. Instrum. Methods Phys. Res., Sect. A **557**, 87 (2006).
[14] C. Limborg-Deprey and P. Bolton, Nucl. Instrum. Methods Phys. Res., Sect. A **557**, 106 (2006).
[15] A. M. Weiner *et al.*, Opt. Lett. **15**, 326 (1990), and references therein.
[16] P. Tournois, Opt. Commun. **140**, 245 (1997); F. Verluise *et al.*, Opt. Lett. **25**, 575 (2000).
[17] See, e.g., *Laser Beam Shaping*, edited by F. M. Dickey and S. C. Holswade (Marcel Dekker, New York, 2000).
[18] R. Piestun and D. Miller, Opt. Lett. **26**, 1373 (2001), and references therein.
[19] M. Born and E. Wolf, *Principles of Optics* (Cambridge University Press, Cambridge, UK, 2003).
[20] M. Kempe, U. Stamm, B. Wilhelmi, and W. Rudolph, J. Opt. Soc. Am. B **9**, 1158 (1992).
[21] J. Hammersley, *Proceedings of the New York Academy of Science*, Vol. 86, p. 844 (1960).
[22] http://www.pulsar.nl/gpt.
[23] M. Ferrario *et al.*, *Proceedings of 2000 European Particle Accelerator Conference, Vienna, Austria* (EPS-IGA, Geneva, 2000), p. 1642.
[24] A. Cianchi *et al.*, *Proceedings of 8th European Workshop on Beam Diagnostics for Particle Accelerators, Venice, Italy*, (ELETTRA, Trieste, 2007), paper WEO2A03.
[25] D. Kaplan (private communication).
[26] D. Dowell *et al.*, *Proceedings of the 29th International Free Electron Laser Conference, Novosibirsk, Russia* (Budker INP, Russia, 2007), paper WEAAU01.
[27] C. Limborg, *Proceedings of the 2002 European Particle Accelerator Conference, Paris, France* (EPS-IGA and CERN, Geneva, 2002), p. 1789.
[28] I. V. Bazarov and C. K. Sinclair, Phys. Rev. ST Accel. Beams **8**, 034202 (2005).